

1

2

3 **Multi-BRCT domain protein Brc1 links Rhp18/Rad18 and  $\gamma$ H2A to maintain**  
4 **genome stability during S-phase**

5

6

7 Michael C. Reubens, Sophie Rozenzhak, and Paul Russell<sup>#</sup>

8

9 Department of Molecular Medicine, The Scripps Research Institute, La Jolla, California

10

11

12

13 Running Head: Rhp18/Rad18 Binds Brc1 to Protect Genome Integrity

14

15 <sup>#</sup>Address correspondence to Paul Russell, [prussell@scripps.edu](mailto:prussell@scripps.edu)

16

17 **ABSTRACT**

18 DNA replication involves the inherent risk of genome instability, as replisomes invariably  
19 encounter DNA lesions or other structures that stall or collapse replication forks during S-phase.  
20 In the fission yeast *Schizosaccharomyces pombe*, the multi-BRCT domain protein Brc1, which is  
21 related to budding yeast Rtt107 and mammalian PTIP, plays an important role in maintaining  
22 genome integrity and cell viability when cells experience replication stress. The C-terminal pair  
23 of BRCT domains in Brc1 were previously shown to bind phospho-histone H2A ( $\gamma$ H2A) formed  
24 by Rad3/ATR checkpoint kinase at DNA lesions; however, the putative scaffold interactions  
25 involving the N-terminal BRCT domains 1-4 of Brc1 have remained obscure. Here we show that  
26 these domains bind Rhp18/Rad18, which is an E3 ubiquitin protein ligase that has crucial  
27 functions in postreplication repair. A missense allele in BRCT domain 4 of Brc1 disrupts binding  
28 to Rhp18 and causes sensitivity to replication stress. Brc1 binding to Rhp18 and  $\gamma$ H2A are  
29 required for the Brc1-overexpression suppression of *smc6-74*, which impairs the Smc5/6  
30 structural maintenance of chromosomes complex required for chromosome integrity and repair  
31 of collapsed replication forks. From these findings we propose that Brc1 provides scaffolding  
32 functions linking  $\gamma$ H2A, Rhp18, and Smc5/6 complex at damaged replication forks.

33

34 **KEYWORDS**

35 Brc1, Rhp18, Rad18, BRCT domain, DNA damage, DNA repair, DNA replication stress,  
36 genome integrity

37

## 38 INTRODUCTION

39 Genome stability is especially at risk during the DNA synthesis (S)-phase of the cell  
40 cycle, when replisomes encounter DNA lesions or chromatin-bound proteins, or they collide with  
41 converging replication or transcriptional machinery, potentially leading to replication fork  
42 collapse and ensuing deleterious genomic alterations. Faced with the critical requirement for  
43 replication fidelity to maintain cell viability and prevent disease (1-3), eukaryotic organisms  
44 have evolved a complex and highly regulated network of DNA damage response (DDR)  
45 pathways that work in conjunction with the replicative machinery to maintain genome integrity  
46 during S-phase (4-8). Thus, DDRs coordinate DNA replication, repair, and cell cycle progression  
47 to safeguard the genome.

48 In *Schizosaccharomyces pombe* (*S. pombe*), as in all eukaryotes, the replication stress  
49 response is initiated by the detection of replication protein a (RPA)-coated single-stranded DNA  
50 (ssDNA) that forms at stalled or damaged replication forks. This accumulation of RPA-bound  
51 ssDNA serves as a signal to activate the master checkpoint kinase Rad3/ATR, which  
52 phosphorylates key substrates including an SQ motif on the C-terminal tail of histone H2A in  
53 chromatin flanking the stalled or collapsed replication fork (9, 10). Phospho-histone H2A,  
54 known as  $\gamma$ H2A in yeast and equivalent to  $\gamma$ H2AX in mammals, serves as a recruitment platform  
55 for key DDR proteins, including Brc1, Crb2, and Mdb1 in *S. pombe* (11-15).

56 Brc1 is an 878-amino acid (aa) protein that contains four N-terminal and two C-terminal  
57 BRCT domains separated by an intervening linker region containing a nuclear localization signal  
58 (Figure 1A) (16). This domain organization is shared with *Saccharomyces cerevisiae* Rtt107 and  
59 mammalian PTIP, which are important genome protection proteins (17-22). Brc1 was first  
60 identified in *S. pombe* as an allele-specific high-copy suppressor of the hypomorphic *smc6-74*

61 allele, which impairs the function of the essential Smc5/6 structural maintenance of  
62 chromosomes complex (23). Brc1 is not required for cell viability unless cells are challenged  
63 with DNA damaging agents that collapse replication forks, or they are defective in specific  
64 processes related to DNA replication. For example, Brc1 is essential for cell viability in mutants  
65 lacking Rqh1, which is a RecQ-like DNA helicase involved in DNA replication and repair (9,  
66 24). Rqh1 is homologous to Sgs1 in *S. cerevisiae* and the BLM, WRN and RTS/RECQ4  
67 enzymes in humans that are associated with cancer predisposition and/or premature aging (25).  
68 Brc1 is also crucial when loss of deoxycytidylate deaminase (dCMP deaminase) creates  
69 imbalanced pools of deoxyribonucleoside triphosphates (dNTPs) required for DNA synthesis and  
70 repair (26), or when there are defects in replication factor c (RFC), which loads proliferating cell  
71 nuclear antigen (PCNA) clamp onto duplex DNA (10). Perhaps most notably, Brc1 becomes  
72 essential in cells with compromised Smc5/6 complex function (23, 24). The reported function of  
73 the Smc5/6 complex at collapsed replication forks (27-29), combined with the observed  
74 sensitivity of Brc1-deficient cells to agents known to generate lesions and disrupt replication fork  
75 progression during S-phase, suggests that Brc1 functions in the response to DNA damage during  
76 replication stress (24). Further supporting this idea, Brc1 was shown to localize at sites of  
77 replication stress through the interaction of its C-terminal BRCT domains with  $\gamma$ H2A (12).  
78 Collectively, these data suggest that Brc1 stabilizes stalled replication forks and assists in the  
79 repair of collapsed replication forks (9, 10, 12, 16, 30).

80       Exactly how Brc1 protects genomic stability during S-phase has remained elusive.  
81 Extensive genetic interaction analysis has established that Brc1 is especially crucial for  
82 replication stress resistance and cell viability when DNA replication or other genome protection  
83 mechanisms are impaired (9, 10, 23, 24, 31-33); however, lack of specific measureable

84 enzymatic activity and limited protein interaction data have hindered progression in  
85 understanding Brc1's role in the maintenance of genomic stability under these circumstances.  
86 Brc1 binds  $\gamma$ H2A, but this interaction probably serves to properly localize Brc1 at DNA lesions,  
87 where it engages with other proteins that are currently unknown. Moreover, mutations that  
88 disrupt Brc1 binding to  $\gamma$ H2A only partially impair Brc1 function, indicating  $\gamma$ H2A-independent  
89 roles for Brc1 that do not absolutely require formation of extensive domains of chromatin-bound  
90 Brc1 flanking stalled or collapsed replication forks (12, 16). The *smc6-74* suppression by Brc1  
91 overexpression was shown to require Rhp18, but whether this dependence reflects physical  
92 associations between Brc1, Rhp18, or the Smc5/6 holocomplex is unknown (24, 31). Rhp18,  
93 known as Rad18 in other organisms, is an E3 ubiquitin protein ligase, which binds RPA-coated  
94 ssDNA, where it functions with its cognate E2 enzyme, Rad6, to control the initial steps of post  
95 replicative repair (PRR) via proliferating cell nuclear antigen (PCNA) ubiquitination (34).

96 In this report, we identify Rhp18 as a binding partner for Brc1 and describe a mutation  
97 that disrupts this interaction. Binding studies and functional analysis suggest the interaction with  
98 Rhp18 is essential for Brc1 overexpression to suppress *smc6-74*. Moreover, Brc1 binding to  
99  $\gamma$ H2A is critical when the function of the Smc5/6 complex is impaired. These results suggest that  
100 Brc1's role in promoting genomic stability during S-phase is mediated through coordinated  
101 binding with  $\gamma$ H2A and Rhp18 at sites of replication stress.

102

## 103 RESULTS

104 **Brc1 physically interacts with Rhp18.** BRCT domains often mediate physical  
105 interactions amongst proteins (35, 36). Brc1 contains six BRCT domains but no documented  
106 enzymatic activity, thus it seemed likely that it functions as a scaffold for other DDR proteins at

107 stalled or damaged replication forks. To date the only interacting partner identified for Brc1 has  
108 been  $\gamma$ H2A (12). Therefore, we sought to identify additional Brc1 interacting proteins through a  
109 yeast two-hybrid (Y2H) screen using full length Brc1 as bait. The results from this preliminary  
110 screen returned multiple hits for Rhp18, which was notable given that Rhp18 is required for the  
111 rescue of *smc6-74* by Brc1 overexpression (24, 31).

112 To confirm these preliminary results, we cloned full length *brc1* cDNA into *pGBKT7* and  
113 full length *rhp18* cDNA into *pGADT7* and assessed their two-hybrid interactions. Rhp18  
114 displayed one-hybrid activity on standard -His selective media (Dex-L-T-H), but addition of 5  
115 mM 3-Amino-1,2,4 Triazole (3-AT) to the media suppressed this activity and confirmed the  
116 Brc1-Rhp18 interaction reported from our initial screen (Figure 1C). These results were later  
117 validated through co-immunoprecipitation, as described below.

118

119 **Identification of domains mediating the Brc1-Rhp18 interaction.** With Rhp18  
120 identified as a binding partner of Brc1, we sought to narrow down the protein domains mediating  
121 this interaction. Fragments of Brc1 were evaluated for their ability to bind full length Rhp18  
122 using the Y2H method (Figure 1A). This analysis revealed that a Brc1 fragment containing  
123 BRCT domains 1-4 plus part of the linker region was sufficient for the Y2H interaction with  
124 Rhp18. However, division of this fragment between the BRCT domains 2 and 3 eliminated the  
125 Y2H signal, suggesting that BRCT domains 1-4 likely function as a binding module for Rhp18  
126 (Figure 1C).

127 Rhp18 is a 387-aa protein that contains an N-terminal really interesting new gene (RING)  
128 domain, a central Mid zinc finger domain, and a C-terminal SAF-A/B, Acinus, Pias (SAP)  
129 domain. The N-terminal RING domain coordinates binding of Rad6, an E2 ubiquitin conjugating

130 enzyme, along with the C-terminal Rad6 binding interface. Aside from coordinating Rad6  
131 binding, the RING domain is known to mediate Rhp18's E3 ubiquitin ligase activity to initiate  
132 PRR pathways (31, 37). The C-terminal SAP domain has been suggested to possess ssDNA-  
133 binding activity, which might recruit Rhp18 to sites of DNA lesions in concert with Rhp18's  
134 ability to bind RPA (38-40). However, the function of the central Mid zinc finger domain is  
135 uncertain, as some reports have claimed it mediates replication-independent DNA binding (38),  
136 while others have shown that this domain functions as a ubiquitin-binding zinc finger (UBZ)  
137 domain (37).

138         To identify the regions of Rhp18 required for its interaction with Brc1, we utilized our  
139 Y2H approach. Fragments of Rhp18 (Figure 1B) were cloned into pGADT7 and tested for their  
140 ability to interact with full length Brc1 or the Brc1(1-4) fragment expressed from pGBKT7  
141 (Figure 1A). Removal of the SAP domain alleviated the observed one-hybrid activity in  
142 pGADT7, and allowed scoring of interactions on restrictive plates lacking 3-AT. The  
143 Rhp18(R/M) fragment supported growth on the restrictive plates, suggesting that the SAP  
144 domain is not essential for the Brc1 interaction (Figure 1D). The N-terminal RING domain failed  
145 to support growth on the restrictive plates when combined with either full length Brc1 or the N-  
146 terminal BRCT domains (Figure 1D), suggesting that the RING domain alone is insufficient to  
147 mediate the interaction with Brc1. The combined results above implied that the Mid domain  
148 alone may be sufficient to interact with Brc1, and the two-hybrid analysis expressing only the  
149 Mid domain in pGADT7 in conjunction with the Brc1 fragments in pGBKT7 corroborated that  
150 assumption (Figure 1D). Therefore, our results suggest the Mid zinc finger domain of Rhp18  
151 alone is sufficient to support the physical interaction with Brc1.

152

153           **Mutation of BRCT domain 4 severely attenuates the Brc1-Rhp18 physical**  
154 **interaction.** Having identified the regions of Brc1 and Rhp18 required for their physical  
155 interaction, we next turned our attention to analyzing the effects of previously characterized  
156 point mutations altering conserved residues in the BRCT domains of Brc1 (12, 16). As expected,  
157 the *brc1-T672A* mutation that disrupts binding to  $\gamma$ H2A did not diminish binding to Rhp18  
158 (Figure 2B). Brc1 proteins with altered residues in BRCT domain 2 (*G136A* and *TH148, 149SG*)  
159 or BRCT domain 3 (*R268K* and *W298F, P301G*) also maintained the Y2H interaction with  
160 Rhp18. In contrast, the *brc1-HYP307-9GFG* allele, which alters 3 residues in BRCT domain 4  
161 near the BRCT 3-4 linker, eliminated the Y2H interaction with Rhp18 (Figure 2B). Importantly,  
162 previous work showed that *brc1-HYP307-9GFG* impaired Brc1 function in genotoxin resistance  
163 without disrupting its ability form  $\gamma$ H2A-dependent nuclear foci (16), suggesting that this allele  
164 disrupted critical scaffolding properties of Brc1.

165           To confirm the yeast-two hybrid assays we performed co-immunoprecipitation  
166 experiments. Utilizing *nmt41* promoter driven expression of N-terminally tagged Rhp18 and  
167 Brc1, we found that 13myc-tagged Rhp18 readily co-precipitated with TAP-tagged Brc1 (Figure  
168 2C, lane 6). In contrast, Rhp18 co-immunoprecipitation with TAP-tagged Brc1-*HYP307-9GFG*  
169 was strongly diminished (Figure 2C, lane 10).

170

171           **Efficient rescue of *brc1Δ* by expression of *brc1-T672A* but not *brc1-HYP307-9GFG*.**

172           With the identification of point mutations of Brc1 that disrupt binding to Rhp18 or  $\gamma$ H2A,  
173 we directly compared the effects of these mutations in determining cellular resistance to DNA  
174 damage. We expressed *brc1*<sup>+</sup>, the Rhp18-binding defective mutant *brc1-HYP307-9GFG*, or the  
175 previously described  $\gamma$ H2A-binding defective mutant *brc1-T672A* (12), from the moderate

176 strength *nmt41* promoter in plasmid pREP41X. As an additional control, we also expressed *brc1-*  
177 *W298F, P301G*, containing mutations in BRCT domain 3, which did not disrupt the Brc1-Rhp18  
178 Y2H interaction (Figure 2B). We found that expression of *brc1*<sup>+</sup>, *brc1-W298F:P301G*, and *brc1-*  
179 *T672A* were all able to fully rescue *brc1Δ* MMS sensitivity (Figure 3A, rows 4, 5, and 7). In  
180 contrast, expression of *brc1-HYP307-9GFG* resulted in an extremely weak rescue of the MMS  
181 phenotype when compared to the vector only control (Figure 3A, row 6). We obtained essentially  
182 the same results when we repeated the experiment in an *htaAQ* genetic background (*hta1-S129A*  
183 *hta2-S128S*) (Figure 3B), which lacks the ability to form  $\gamma$ H2A (11). Thus, defects in Brc1  
184 binding to  $\gamma$ H2A can be suppressed by Brc1 overexpression; however, the impacts of the Rhp18-  
185 binding defective *brc1-HYP307-9GFG* mutation on Brc1 function cannot be compensated for by  
186 merely increasing its cellular concentrations.

187

188 **Brc1 binding to Rhp18 and  $\gamma$ H2A are important for suppression of *smc6-74* by Brc1**  
189 **overexpression.** We next investigated the relationships between Brc1 binding to  $\gamma$ H2A or Rhp18  
190 and its ability to rescue *smc6-74*. Utilizing the same approach as described above, we expressed  
191 the *brc1* alleles from pREP41X in the *smc6-74* genetic background and tested MMS sensitivity.  
192 As seen for the *brc1Δ* rescue experiments, expression of *brc1*<sup>+</sup> or *brc1-W298F, P301G* fully  
193 suppressed the *smc6-74* MMS-sensitive phenotype in these assays (Figure 4A, rows 4-5). In  
194 contrast, expression of *brc1-HYP307-9GFG* resulted in no suppression of *smc6-74* (Figure 4A,  
195 row 6). The correlation of attenuated Rhp18 binding and lack of *smc6-74* suppression observed  
196 for *brc1-HYP307-9GFG* overexpression suggests that binding to Rhp18 is critical for Brc1  
197 function. Interestingly, suppression *smc6-74* by *brc1-T672A* overexpression was weakened in

198 comparison to *brc1*<sup>+</sup> overexpression (Figure 4A, row 7), suggesting that  $\gamma$ H2A-binding by Brc1  
199 is important for suppression of *smc6-74*.

200 To further investigate whether binding to  $\gamma$ H2A is important for the Brc1 overexpression  
201 rescue of *smc6-74*, we assessed the ability of our *brc1* alleles to suppress *smc6-74* in an *htaAQ*  
202 background. Importantly, combining the *smc6-74* and *htaAQ* mutations in the same strain caused  
203 an apparent synergistic increase in MMS sensitivity (compare Figure 4A, row 3 to Figure 4B,  
204 rows 1 and 3). Expression of *brc1*<sup>+</sup> or *brc1-W298F, P301G* suppressed the *smc6-74* MMS-  
205 sensitive phenotype, but MMS-resistance was diminished in the *htaAQ* background (compare  
206 Figures 4A-B, rows 4-5). As expected, an approximately equal level of suppression was  
207 observed for *brc1-T672A* overexpression in the *htaAQ* background (Figure 4B, row 7), and no  
208 suppression was observed for *brc1-HYP307-9GFG* overexpression (Figure 4B, row 6).

209 These results suggest that interactions of Brc1 with  $\gamma$ H2A and Rhp18 are important for  
210 suppression of *smc6-74* by Brc1 overexpression. To further test this hypothesis, we examined  
211 suppression in the *htaAQ rhp18 $\Delta$  smc6-74* genetic background. As expected, Brc1  
212 overexpression only weakly suppressed MMS sensitivity of *htaAQ rhp18 $\Delta$  smc6-74* cells (Figure  
213 4C). This very weak suppression effect was observed for *brc1*<sup>+</sup>, *brc1-W298F, P301G* and *brc1-*  
214 *T672A* overexpression. However, this weak suppression was eliminated when we over-expressed  
215 *brc1-HYP307-9GFG* (Figure 4C, row 6). This result implies that the *smc6-74* suppression defect  
216 of *brc1-HYP307-9GFG* is not fully explained by its inability to interact with Rhp18.

217

## 218 **DISCUSSION**

219 Two-thirds of the mutations associated with human cancers arise from DNA replication  
220 errors, emphasizing the need to understand how cells protect genome integrity during S-phase

221 (1). Brc1 preserves genomic stability in response to replication stress, but the mechanism has  
222 remained elusive (23, 24, 31-33). One well-defined property of Brc1 is its ability to bind  $\gamma$ H2A  
223 through its C-terminal BRCT domains. In this report, we have identified Rhp18 as another  
224 binding partner of Brc1. This interaction is mediated through the N-terminal region of Brc1  
225 containing BRCT domains 1-4 and it was disrupted by the *brc1-HYP307-9GFG* allele containing  
226 clustered mutations at the beginning of BRCT domain 4. As observed for wild type Brc1, the  
227 Brc1 protein encoded by *brc1-HYP307-9GFG* properly localizes in the nucleus, where it forms  
228 foci in response to replication stress (16). Thus, the *brc1-HYP307-9GFG* mutation does not  
229 appear to grossly disrupt Brc1 protein stability or localization, or its ability to bind  $\gamma$ H2A-marked  
230 chromatin flanking stalled or damaged replication forks. From these results, we propose that the  
231 *brc1-HYP307-9GFG* mutation most likely disrupts a scaffolding function of Brc1 that involves  
232 binding Rhp18. This model is consistent with the requirements for Rhp18 to tolerate genotoxins  
233 that cause replication fork stalling and collapse, and the requirement for Rhp18 in suppression of  
234 *smc6-74* by Brc1 overexpression (24, 31). Importantly, the *brc1-HYP307-9GFG* mutation  
235 abrogates *smc6-74* suppression by Brc1 overexpression.

236 As a technical note, we used the yeast two-hybrid method for our studies because we  
237 could not reliably precipitate full-length Brc1 in non-denaturing buffers. However, as shown in  
238 Figure 2C, we have largely solved this problem through the use of an N-terminal TAP tag,  
239 although a substantial amount of Brc1 appears to still be proteolytically cleaved. Importantly, we  
240 could confirm our two-hybrid findings with these co-immunoprecipitation studies. The ability to  
241 precipitate TAP-tagged Brc1 in non-denaturing buffers will make it possible to employ  
242 proteomic methods in future experiments, which has been a very profitable strategy for analyzing  
243 the function of Rtt107 (21).

244 We observed that suppression of *smc6-74* MMS sensitivity by Brc1 overexpression is  
245 largely ablated when Brc1 cannot bind to  $\gamma$ H2A. Moreover, elimination of  $\gamma$ H2A strongly  
246 sensitizes *smc6-74* cells to MMS. These data strengthen the evidence linking Brc1 to the  
247 proposed role for the Smc5/6 complex in homologous recombination (HR)-mediated repair of  
248 stalled replication forks (27-29). One possibility is that diminished Smc5/6 function creates a  
249 greater demand for Brc1 to act in fork stabilization and potential channeling of fork repair, or  
250 resolution, through alternate pathways that likely depend on Mus81-Eme1 or Slx1-Slx4 (24, 41,  
251 42).

252 It has been reported that Rhp18 is recruited to ssDNA and RPA-bound ssDNA (39, 40).  
253 Given that RPA bound to ssDNA is sensed by Rad3/ATR, which phosphorylates H2A to form  
254  $\gamma$ H2A (5, 43), it is unlikely that Rhp18 localization at DNA lesions requires binding to Brc1.  
255 However, the potential presence of Rhp18 at the site of stalled replication forks, through its  
256 interaction with RPA, could provide a potential binding surface at the fork to explain the  $\gamma$ H2A-  
257 independent function for Brc1 that has been suggested in previous publications (12, 16).

258 It was previously reported that the dependence of the *smc6-74* rescue on Rhp18 was due  
259 to a requirement for the translesion synthesis (TLS) branch of PRR at higher MMS doses;  
260 however, the requirement at lower MMS concentrations could not be attributed to a known  
261 function of Rhp18 (24, 31). The results presented here combined with previously published data  
262 suggesting that RPA-coated ssDNA can negatively regulate Rad51 strand invasion (44-46),  
263 suggest the potential for the binding of Brc1 to RPA-bound Rhp18 to stabilize RPA on its ssDNA  
264 substrate, thus potentially inhibiting HR-mediated fork resolution. In the presence of a low level  
265 of DNA alkylation damage this stabilization of RPA could serve to inhibit Rad51 strand invasion,  
266 therefore inhibiting the onset of HR-mediated fork resolution and allowing excision pathways to

267 repair alkylated bases. This idea would be consistent with the requirement for Rhp18 in the  
268 *smc6-74* rescue in response to low level MMS treatment, accompanied by no known Rhp18  
269 activity under those circumstances (31). Furthermore, the interaction between Brc1 and RPA  
270 bound Rhp18 would allow for the process of TLS to be mediated at MMS doses that can be  
271 tolerated by this method of PRR. Under this scenario, it is also possible that in response to high  
272 accumulation of alkylated bases that cannot be repaired via the previously mentioned  
273 mechanisms, the fork could be held in a stable confirmation while Brc1 mediates the firing of  
274 surrounding dormant replication origins in an Orc1 dependent manner (47), allowing the  
275 resolution of the stalled fork via HR-mediated pathways late in S-phase or possibly in G2. If this  
276 hypothetical series of events are correct it could potentially explain the complex epistatic  
277 relationships between Brc1 and factors involved in multiple DDR pathways (23, 24, 31-33).

278 Finally, we note that a recent proteomics study with human cells led to the discovery of a  
279 putative DNA repair factor, consisting of SLF1 and SLF2, which physically links Smc5/6  
280 complex to Rad18 bound to RNF168-catalyzed ubiquitin chains at certain types of DNA lesions  
281 (48). SLF1, also known as BRCTx, is a multi-BRCT domain protein that uses its BRCT domains  
282 to bind Rad18 (49, 50). Indeed, this SLF1/BRCTx-Rad18 interaction was first discovered  
283 through a two-hybrid screen that used BRCTx as bait, just as we discovered the Brc1-Rhp18  
284 interaction in fission yeast. The protein interaction network involving SLF1/SLF2, Rad18 and  
285 Smc5/6 complex does not include Rad6, suggesting that Rad18 functions structurally and not  
286 catalytically in this network (48). Strikingly, suppression of *smc6-74* by Brc1 overexpression on  
287 low dose MMS does not require Rhp6, the fission yeast ortholog of Rad6 (31). Rtt107, the Brc1-  
288 like protein in budding yeast, was shown to mediate Smc5/6 recruitment to DSBs (51). Thus,  
289 there appear to be several striking parallels of protein interactions involving Brc1/Rtt107/PTIP

290 BRCT domain proteins, Rad18/Rhp18, and the Smc5/6 complex. We look forward to learning  
291 whether these similarities reflect evolutionary divergence of a conserved mechanism of  
292 localizing Smc5/6 complex to DNA lesions.

293

## 294 MATERIALS AND METHODS

295 ***S. pombe* cultivation and general methods.** Standard *S. pombe* methods were conducted  
296 as previously described (52), and all *S. pombe* strains used in this study are listed in Table 1. The  
297 *rhp18Δ* strain was generated using a targeting construct that replaced the entire *rhp18*<sup>+</sup> open  
298 reading frame with a hygromycin B (*hphMX6*) cassette, and Rhp18 was N-terminally tagged at  
299 its endogenous locus using pFA6-*natMX6-p41nmt-13myc* (described below) using described  
300 methods (53). Both the deletion of Rhp18 and the epitope tag were subsequently verified by PCR  
301 and sequencing before use in any experiments. Double and triple mutants were generated using  
302 random spore analysis, the resulting genotypes were validated by growth on appropriate selective  
303 media, and then subsequently verified by PCR.

304 For immunoprecipitation experiments, exponentially growing cultures of indicated strains  
305 were cultivated in appropriately supplemented Edinburgh Minimal Media (EMM2) in the  
306 presence, or absence, of 5 μg/mL thiamine for 25 hours at 30°C to actively regulate the  
307 expression from the *nmt41* promoter. For MMS survival assays the indicated strains were  
308 cultivated in appropriately supplemented EMM2 media in the presence of 5 μg/mL thiamine for  
309 25 hours, log phase cultures were then suspended to 0.4 OD<sub>600</sub> and serially diluted five-fold onto  
310 yeast extract, glucose, and supplements (YES) agar plates containing the designated  
311 concentration of MMS. Cell growth was evaluated after 4 days at 30°C as previously described  
312 (24, 31).

313

314           **Plasmid construction.** For the Y2H analysis constructs, all *brc1* fragments (**FL**: 1-  
315 878aa, **1-4**: 1-553aa, **1-2**: 1-202aa, and **3-4**: 195-553aa), and point mutants, were isolated using  
316 standard PCR methods with NdeI linkers on upstream primers and BamHI linkers on  
317 downstream primers. All *rhp18* fragments (**FL**: 1-387aa, **R/M**: 1-202aa, **R**: 1-117aa, and **M**:  
318 111-202aa) were generated using a similar PCR mediated strategy except for using XmaI linkers  
319 on the downstream primers. The resulting *brc1* inserts were then ligated into NdeI and BamHI  
320 digested pGBKT7, and the *rhp18* fragments were ligated into NdeI and XmaI digested pGADT7.  
321 Expression of TAP-Brc1 was achieved by cloning full length *brc1*<sup>+</sup>, or *brc1-HYP307-9GFG*,  
322 cDNA into NdeI and BamHI digested pREP41-NTAP as previously described (54). For MMS  
323 survival assays pREP41X*brc1*<sup>+</sup> was used to rescue the MMS phenotypes as previously described  
324 (24, 31), and all evaluated *brc1* point mutants were generated by site-directed mutagenesis  
325 (Agilent Technologies) using pREP41X*brc1*<sup>+</sup> as template. To N-terminally tag Rhp18 at its  
326 endogenous locus pFA6a-natMX6-p41*nmt*-13myc was constructed by cleaving the 3XFLAG  
327 from pFA6a-natMX6-p41*nmt*-3XFLAG (55) and replacing it with the 13myc tag, without its stop  
328 codon, isolated from pFA6a-13myc-natMX6 (53). All plasmids generated for use in this study  
329 were sequence verified before use.

330

331           **Yeast two-hybrid analysis.** All Brc1 and Rhp18 fusion constructs were generated as  
332 described above. The resulting fusion protein constructs were transformed into the *S. cerevisiae*  
333 AH109 reporter strain (Clontech Matchmaker<sup>®</sup> Gold System), and co-transformants were  
334 selected for by plating on Dex-L-T media. Y2H analysis was carried out by diluting the indicated  
335 log phase cultures to an OD<sub>600</sub> of 0.4 and then spotting them onto restrictive and permissive

336 plates. Control growth was evaluated on Dex-L-T and protein interactions were scored either  
337 Dex-L-T-H with, or without, 3-AT based on the presence of one-hybrid activity. All Y2H growth  
338 was scored after three days of growth at 32°C.

339

340 **Immunoblotting and immunoprecipitation.** Whole cell extracts (WCE) were generated  
341 from 15 mL cultures of the indicated strains cultivated as described above. Cell pellets were  
342 lysed in lysis buffer (50 mM Tris pH 8.0, 150mM NaCl, 5 mM EDTA, 10% glycerol, 0.1%  
343 Nonidet-P40, 1 mM NaF, 1 mM PMSF, and Complete Protease Inhibitors) using a FastPrep<sup>®</sup>-24  
344 (MP Biomedicals) following the manufacturer's protocol. For each lysate 1.5 mg total protein  
345 was incubated with rabbit IgG (Sigma) conjugated Dynabeads<sup>®</sup> M-280 Tosylactivated (Thermo  
346 Fisher Scientific) for three hours at 4°C with rotation. The beads were collected and washed  
347 three times in lysis buffer before eluting the proteins from the beads by boiling in 1xSDS-PAGE  
348 loading buffer (100mM Tris pH6.8, 4% SDS, 20% glycerol, and 0.2% Bromophenol blue).  
349 Proteins were resolved on Novex WedgeWell 4-20% Tris-Glycine gels (Thermo Fisher  
350 Scientific), transferred via iBlot2<sup>®</sup> (Thermo Fisher Scientific) to nitrocellulose membranes, and  
351 blocked and probed using standard techniques and manufacturer's recommended protocols.  
352 TAP-Brc1 was detected using Peroxidase anti-peroxidase (PAP) soluble complex antibody  
353 produced in rabbit (P12291, Sigma-Aldrich) diluted 1:2,000, 13myc-Rhp18 was detected using  
354 anti-myc antibody (9E10, Covance) diluted 1;1,000, and tubulin was detected using monoclonal  
355 anti- $\alpha$ -Tubulin antibody produced in mouse (T5168, Sigma-Aldrich) diluted 1:10,000.

356

357 **ACKNOWLEDGEMENTS**

358 We thank Matthew O’Connell for plasmids and technical insights, Oliver Limbo for  
359 technical support, and members of the Russell laboratory and Nick Boddy for helpful  
360 discussions.

361 This research was supported by NIH grants GM059347, CA077325 and CA117638 to  
362 P.R.

363 We declare no conflicts of interest.

364

## 365 REFERENCES

- 366 1. **Tomasetti C, Li L, Vogelstein B.** 2017. Stem cell divisions, somatic mutations, cancer etiology,  
367 and cancer prevention. *Science* **355**:1330.
- 368 2. **Tubbs A, Nussenzweig A.** 2017. Endogenous DNA Damage as a Source of Genomic Instability in  
369 Cancer. *Cell* **168**:644-656.
- 370 3. **Aguilera A, Garcia-Muse T.** 2013. Causes of genome instability. *Annu Rev Genet* **47**:1-32.
- 371 4. **Gadaleta MC, Noguchi E.** 2017. Regulation of DNA Replication through Natural Impediments in  
372 the Eukaryotic Genome. *Genes (Basel)* **8**.
- 373 5. **Branzei D, Foiani M.** 2009. The checkpoint response to replication stress. *DNA Repair* **8**:1038-  
374 1046.
- 375 6. **Cortez D.** 2015. Preventing replication fork collapse to maintain genome integrity. *DNA Repair*  
376 (Amst) **32**:149-157.
- 377 7. **Iyer DR, Rhind N.** 2017. The Intra-S Checkpoint Responses to DNA Damage. *Genes (Basel)* **8**.
- 378 8. **Branzei D, Foiani M.** 2010. Maintaining genome stability at the replication fork. *Nat Rev Mol Cell*  
379 *Biol* **11**:208-219.

- 380 9. **Rozenzhak S, Mejía-Ramírez E, Williams JS, Schaffer L, Hammond JA, Head SR, Russell P.** 2010.  
381 Rad3ATR Decorates Critical Chromosomal Domains with  $\gamma$ H2A to Protect Genome Integrity  
382 during S-Phase in Fission Yeast. *PLOS Genetics* **6**:e1001032.
- 383 10. **Mejia-Ramirez E, Limbo O, Langerak P, Russell P.** 2015. Critical Function of  $\gamma$ H2A in S-Phase.  
384 *PLOS Genetics* **11**:e1005517.
- 385 11. **Nakamura TM, Du L-L, Redon C, Russell P.** 2004. Histone H2A Phosphorylation Controls Crb2  
386 Recruitment at DNA Breaks, Maintains Checkpoint Arrest, and Influences DNA Repair in Fission  
387 Yeast. *Molecular and Cellular Biology* **24**:6215-6230.
- 388 12. **Williams JS, Williams RS, Dovey CL, Guenther G, Tainer JA, Russell P.** 2010.  $\gamma$ H2A binds Brc1 to  
389 maintain genome integrity during S-phase. *The EMBO Journal* **29**:1136-1148.
- 390 13. **Du LL, Nakamura TM, Russell P.** 2006. Histone modification-dependent and -independent  
391 pathways for recruitment of checkpoint protein Crb2 to double-strand breaks. *Genes Dev*  
392 **20**:1583-1596.
- 393 14. **Sofueva S, Du LL, Limbo O, Williams JS, Russell P.** 2010. BRCT domain interactions with  
394 phospho-histone H2A target Crb2 to chromatin at double-strand breaks and maintain the DNA  
395 damage checkpoint. *Mol Cell Biol* **30**:4732-4743.
- 396 15. **Wei Y, Wang HT, Zhai Y, Russell P, Du LL.** 2014. Mdb1, a fission yeast homolog of human MDC1,  
397 modulates DNA damage response and mitotic spindle function. *PLoS One* **9**:e97028.
- 398 16. **Lee SY, Russell P.** 2013. Brc1 links replication stress response and centromere function. *Cell*  
399 *Cycle* **12**:1665-1671.
- 400 17. **Hang LE, Peng J, Tan W, Szakal B, Menolfi D, Sheng Z, Lobachev K, Branzei D, Feng W, Zhao X.**  
401 2015. Rtt107 Is a Multi-functional Scaffold Supporting Replication Progression with Partner  
402 SUMO and Ubiquitin Ligases. *Mol Cell* **60**:268-279.

- 403 18. **Wan B, Hang LE, Zhao X.** 2016. Multi-BRCT scaffolds use distinct strategies to support genome  
404 maintenance. *Cell Cycle* **15**:2561-2570.
- 405 19. **Leung GP, Brown JA, Glover JN, Kobor MS.** 2016. Rtt107 BRCT domains act as a targeting  
406 module in the DNA damage response. *DNA Repair (Amst)* **37**:22-32.
- 407 20. **Balint A, Kim T, Gallo D, Cussiol JR, Bastos de Oliveira FM, Yimit A, Ou J, Nakato R, Gurevich A,**  
408 **Shirahige K, Smolka MB, Zhang Z, Brown GW.** 2015. Assembly of Slx4 signaling complexes  
409 behind DNA replication forks. *EMBO J* **34**:2182-2197.
- 410 21. **Ohouo PY, Bastos de Oliveira FM, Almeida BS, Smolka MB.** 2010. DNA damage signaling  
411 recruits the Rtt107-Slx4 scaffolds via Dpb11 to mediate replication stress response. *Mol Cell*  
412 **39**:300-306.
- 413 22. **Ray Chaudhuri A, Callen E, Ding X, Gogola E, Duarte AA, Lee JE, Wong N, Lafarga V, Calvo JA,**  
414 **Panzarino NJ, John S, Day A, Crespo AV, Shen B, Starnes LM, de Ruiter JR, Daniel JA,**  
415 **Konstantinopoulos PA, Cortez D, Cantor SB, Fernandez-Capetillo O, Ge K, Jonkers J, Rottenberg**  
416 **S, Sharan SK, Nussenzweig A.** 2016. Replication fork stability confers chemoresistance in BRCA-  
417 deficient cells. *Nature* **535**:382-387.
- 418 23. **Verkade HM, Bugg SJ, Lindsay HD, Carr AM, O'Connell MJ.** 1999. Rad18 Is Required for DNA  
419 Repair and Checkpoint Responses in Fission Yeast. *Molecular Biology of the Cell* **10**:2905-2918.
- 420 24. **Sheedy DM, Dimitrova D, Rankin JK, Bass KL, Lee KM, Tapia-Alveal C, Harvey SH, Murray JM,**  
421 **O'Connell MJ.** 2005. Brc1-Mediated DNA Repair and Damage Tolerance. *Genetics* **171**:457-468.
- 422 25. **Bernstein KA, Gangloff S, Rothstein R.** 2010. The RecQ DNA helicases in DNA repair. *Annu Rev*  
423 *Genet* **44**:393-417.
- 424 26. **Sanchez A, Sharma S, Rozenzhak S, Roguev A, Krogan NJ, Chabes A, Russell P.** 2012. Replication  
425 fork collapse and genome instability in a deoxycytidylate deaminase mutant. *Mol Cell Biol*  
426 **32**:4445-4454.

- 427 27. **Pebernard S, McDonald WH, Pavlova Y, Yates JR, Boddy MN.** 2004. Nse1, Nse2, and a Novel  
428 Subunit of the Smc5-Smc6 Complex, Nse3, Play a Crucial Role in Meiosis. *Molecular Biology of*  
429 *the Cell* **15**:4866-4876.
- 430 28. **Morikawa H, Morishita T, Kawane S, Iwasaki H, Carr AM, Shinagawa H.** 2004. Rad62 Protein  
431 Functionally and Physically Associates with the Smc5/Smc6 Protein Complex and Is Required for  
432 Chromosome Integrity and Recombination Repair in Fission Yeast. *Molecular and Cellular*  
433 *Biology* **24**:9401-9413.
- 434 29. **Pebernard S, Wohlschlegel J, McDonald WH, Yates JR, Boddy MN.** 2006. The Nse5-Nse6 Dimer  
435 Mediates DNA Repair Roles of the Smc5-Smc6 Complex. *Molecular and Cellular Biology* **26**:1617-  
436 1630.
- 437 30. **Lee SY, Rozenzhak S, Russell P.** 2013.  $\gamma$ H2A-Binding Protein Brc1 Affects Centromere Function in  
438 Fission Yeast. *Molecular and Cellular Biology* **33**:1410-1416.
- 439 31. **Lee KM, Nizza S, Hayes T, Bass KL, Irmisch A, Murray JM, O'Connell MJ.** 2007. Brc1-Mediated  
440 Rescue of Smc5/6 Deficiency: Requirement for Multiple Nucleases and a Novel Rad18 Function.  
441 *Genetics* **175**:1585-1595.
- 442 32. **Sánchez A, Roguev A, Krogan NJ, Russell P.** 2015. Genetic Interaction Landscape Reveals Critical  
443 Requirements for *Schizosaccharomyces pombe* Brc1 in DNA Damage Response Mutants. *G3:*  
444 *Genes|Genomes|Genetics* **5**:953.
- 445 33. **Sánchez A, Russell P.** 2015. Ku Stabilizes Replication Forks in the Absence of Brc1. *PLOS ONE*  
446 **10**:e0126598.
- 447 34. **Gao Y, Mutter-Rottmayer E, Zlatanou A, Vaziri C, Yang Y.** 2017. Mechanisms of Post-Replication  
448 DNA Repair. *Genes* **8**:64.
- 449 35. **Leung CCY, Glover JNM.** 2011. BRCT domains: Easy as one, two, three. *Cell Cycle* **10**:2461-2470.

- 450 36. **Reinhardt HC, Yaffe MB.** 2013. Phospho-Ser/Thr-binding domains: navigating the cell cycle and  
451 DNA damage response. *Nat Rev Mol Cell Biol* **14**:563-580.
- 452 37. **Notenboom V, Hibbert RG, van Rossum-Fikkert SE, Olsen JV, Mann M, Sixma TK.** 2007.  
453 Functional characterization of Rad18 domains for Rad6, ubiquitin, DNA binding and PCNA  
454 modification. *Nucleic Acids Research* **35**:5819-5830.
- 455 38. **Nakajima S, Lan L, Kanno S-i, Usami N, Kobayashi K, Mori M, Shiomi T, Yasui A.** 2006.  
456 Replication-dependent and -independent Responses of RAD18 to DNA Damage in Human Cells.  
457 *Journal of Biological Chemistry* **281**:34687-34695.
- 458 39. **Huttner D, Ulrich HD.** 2008. Cooperation of replication Protein A with the ubiquitin ligase Rad18  
459 in DNA damage bypass. *Cell Cycle* **7**:3629-3633.
- 460 40. **Davies AA, Huttner D, Daigaku Y, Chen S, Ulrich HD.** 2008. Activation of Ubiquitin-Dependent  
461 DNA Damage Bypass Is Mediated by Replication Protein A. *Molecular Cell* **29**:625-636.
- 462 41. **Froget B, Blaisonneau J, Lambert S, Baldacci G.** 2008. Cleavage of Stalled Forks by Fission Yeast  
463 Mus81/Eme1 in Absence of DNA Replication Checkpoint. *Molecular Biology of the Cell* **19**:445-  
464 456.
- 465 42. **Roseaulin L, Yamada Y, Tsutsui Y, Russell P, Iwasaki H, Arcangioli B.** 2008. Mus81 is essential  
466 for sister chromatid recombination at broken replication forks. *The EMBO Journal* **27**:1378-1387.
- 467 43. **Branzei D, Foiani M.** 2008. Regulation of DNA repair throughout the cell cycle. *Nat Rev Mol Cell*  
468 *Biol* **9**:297-308.
- 469 44. **Dou H, Huang C, Singh M, Carpenter PB, Yeh ETH.** 2010. Regulation of DNA Repair through De-  
470 SUMOylation and SUMOylation of Replication Protein A Complex. *Molecular cell* **39**:333-345.
- 471 45. **Heyer W-D, Ehmsen KT, Liu J.** 2010. Regulation of homologous recombination in eukaryotes.  
472 *Annual review of genetics* **44**:113-139.

- 473 46. **Li X, Heyer W-D.** 2008. Homologous recombination in DNA repair and DNA damage tolerance.  
474 Cell research **18**:99-113.
- 475 47. **Bass KL, Murray JM, Connell MJ.** 2012. Brc1-dependent recovery from replication stress. Journal  
476 of Cell Science **125**:2753.
- 477 48. **Raschle M, Smeenk G, Hansen RK, Temu T, Oka Y, Hein MY, Nagaraj N, Long DT, Walter JC,**  
478 **Hofmann K, Storchova Z, Cox J, Bekker-Jensen S, Mailand N, Mann M.** 2015. DNA repair.  
479 Proteomics reveals dynamic assembly of repair complexes during bypass of DNA cross-links.  
480 Science **348**:1253671.
- 481 49. **Adams DJ, van der Weyden L, Gergely FV, Arends MJ, Ng BL, Tannahill D, Kanaar R, Markus A,**  
482 **Morris BJ, Bradley A.** 2005. BRCTx is a novel, highly conserved RAD18-interacting protein. Mol  
483 Cell Biol **25**:779-788.
- 484 50. **Liu T, Chen H, Kim H, Huen MS, Chen J, Huang J.** 2012. RAD18-BRCTx interaction is required for  
485 efficient repair of UV-induced DNA damage. DNA Repair (Amst) **11**:131-138.
- 486 51. **Leung GP, Lee L, Schmidt TI, Shirahige K, Kobor MS.** 2011. Rtt107 is required for recruitment of  
487 the SMC5/6 complex to DNA double strand breaks. J Biol Chem **286**:26250-26257.
- 488 52. **Forsburg SL, Rhind N.** 2006. Basic Methods for Fission Yeast. Yeast (Chichester, England) **23**:173-  
489 183.
- 490 53. **Bahler J, Wu JQ, Longtine MS, Shah NG, McKenzie A, 3rd, Steever AB, Wach A, Philippsen P,**  
491 **Pringle JR.** 1998. Heterologous modules for efficient and versatile PCR-based gene targeting in  
492 Schizosaccharomyces pombe. Yeast **14**:943-951.
- 493 54. **Tasto JJ, Carnahan RH, Hayes McDonald W, Gould KL.** 2001. Vectors and gene targeting  
494 modules for tandem affinity purification in Schizosaccharomyces pombe. Yeast **18**:657-662.
- 495 55. **Noguchi C, Garabedian MV, Malik M, Noguchi E.** 2008. A vector system for genomic FLAG  
496 epitope-tagging in Schizosaccharomyces pombe. Biotechnology Journal **3**:1280-1285.

497

498 **FIGURE LEGENDS AND TABLES**

499

500 **Figure 1: The Brc1-Rhp18 interaction requires the N-terminal BRCT domains of Brc1 and**

501 **the Mid domain of Rhp18. A and B.** Schematic representations of Brc1 (A) and Rhp18 (B)

502 fragments tested for physical interactions by yeast two-hybrid analysis (fragments sizes for both

503 Brc1 and Rhp18 are listed in the materials and methods section). The location of Brc1's nuclear

504 localization signal is depicted by the green box in A. C. Yeast two-hybrid results showing full

505 length Brc1 and BRCT domains 1-4 interact with full length Rhp18. Interactions were judged

506 from the Dex-L-T-H+5mM 3AT due to observed one-hybrid activity of full length Rhp18 in

507 pGADT7 on Dex-L-T-H. D. Yeast two-hybrid results indicating Rhp18's Mid domain is

508 sufficient to support the interaction with Brc1. Interactions for full length Rhp18 were evaluated

509 from the Dex-L-T-H+5mM3AT due to observed one-hybrid activity of full length Rhp18 in

510 pGADT7 on Dex-L-T-H. Removal of the SAP domain of Rhp18 alleviated the observed one-

511 hybrid activity, allowing assessment of physical interactions on Dex-L-T-H for the R/M, R, and

512 M fragments of Rhp18.

513

514 **Figure 2. Mutation of BRCT domain 4 attenuates the Brc1-Rhp18 interaction. A. A**

515 schematic representation of published Brc1 point mutations (Lee and Russell, 2013) tested for

516 physical interaction with the Mid domain of Rhp18 by yeast two-hybrid analysis.

517 **B.** Yeast two-hybrid results indicating that mutation of BRCT4 inhibits the interaction with the

518 Mid domain of Rhp18. C. Results from co-immunoprecipitation experiments demonstrating the

519 interaction between full length Brc1 and Rhp18, as well as the reduction in Rhp18 binding  
520 observed with TAP-Brc1-HYP307-9GFG versus TAP-Brc1.

521

522 **Figure 3. Efficient rescue of *brc1Δ* by expression of *brc1-T672A* but not *brc1-HYP307-***

523 **9GFG.** A. Functional evaluation of four *brc1* alleles in response to MMS treatment in a *brc1Δ*

524 genetic background suggests that *brc1-HYP307-9GFG* (Lee and Russell, 2013) retains more

525 activity than *brc1Δ*, but significantly less than the previously published  $\gamma$ H2A binding mutant

526 *brc1-T672A* (Williams, J., *et.al.*, 2010), which rescued *brc1Δ* as well as *brc1<sup>+</sup>* and *brc1-W298F*,

527 *P301G*. B. Functional evaluation of the *brc1* alleles in response to MMS treatment in the *htaAQ*

528 *brc1Δ* genetic background, demonstrating the Brc1-Rhp18 interaction is more essential for Brc1

529 function in an overexpression situation than its ability to bind  $\gamma$ H2A.

530

531 **Figure 4. Rhp18 and  $\gamma$ H2A binding are required for efficient rescue of *smc6-74* by Brc1**

532 **overexpression.** A. Results from *smc6-74* suppression experiments comparing the rescue

533 efficiency of the four *brc1* alleles. The *brc1-HYP307-9GFG* allele that disrupts Brc1 binding to

534 Rhp18 prevents Brc1 overexpression suppression of *smc6-74*. The *brc1-T672A* mutation that

535 abrogates binding to  $\gamma$ H2A impairs Brc1 overexpression suppression of *smc6-74*. B. Results

536 from *smc6-74 htaAQ* suppression experiments comparing the four *brc1* mutations, supporting the

537 MMS dose dependence for  $\gamma$ H2A binding in mediating the *smc6-74* rescue by Brc1. C. Results

538 from *brc1* overexpression assays in the *smc6-74 htaAQ rhp18Δ* background, suggesting the

539 failure of *brc1-HYP307-9GFG* to rescue *smc6-74* is not completely explained by its inability to

540 bind Rhp18.

541

542

**Table 1: Table of strains generated for and used in this study**

Lab ID	Genotype (all strains are leu1-32 and ura4-D18)
MR5456	<i>h<sup>-</sup> + pREP41X</i>
MR5457	<i>h<sup>-</sup> + pREP41Xbrc1<sup>+</sup></i>
MR5458	<i>h<sup>-</sup> brc1::kanMX6 + pREP41X</i>
MR5459	<i>h<sup>-</sup> brc1::kanMX6 + pREP41Xbrc1<sup>+</sup></i>
MR5460	<i>h<sup>-</sup> brc1::kanMX6 + pREP41Xbrc1-W298F, P01G</i>
MR5461	<i>h<sup>-</sup> brc1::kanMX6 + pREP41Xbrc1-HYP307-9GFG</i>
MR5462	<i>h<sup>-</sup> brc1::kanMX6 + pREP41Xbrc1-T672A</i>
MR5464	<i>h<sup>-</sup> smc6-74 + pREP41X</i>
MR5465	<i>h<sup>-</sup> smc6-74 + pREP41Xbrc1<sup>+</sup></i>
MR5466	<i>h<sup>-</sup> smc6-74 + pREP41Xbrc1-W298F, P01G</i>
MR5467	<i>h<sup>-</sup> smc6-74 + pREP41Xbrc1-HYP307-9GFG</i>
MR5468	<i>h<sup>-</sup> smc6-74 + pREP41Xbrc1-T672A</i>
MR5469	<i>h<sup>-</sup> hta1-S129A:ura4<sup>+</sup> hta2-S128A:his3<sup>+</sup> his3-D1 + pREP41X</i>
MR5470	<i>h<sup>-</sup> hta1-S129A:ura4<sup>+</sup> hta2-S128A:his3<sup>+</sup> his3-D1 + pREP41XBrc1<sup>+</sup></i>
MR5471	<i>h<sup>-</sup> hta1-S129A:ura4<sup>+</sup> hta2-S128A:his3<sup>+</sup> brc1::kanMX6 his3-D1 + pREP41X</i>
MR5472	<i>h<sup>-</sup> hta1-S129A:ura4<sup>+</sup> hta2-S128A:his3<sup>+</sup> brc1::kanMX6 his3-D1 + pREP41XBrc1<sup>+</sup></i>
MR5473	<i>h<sup>-</sup> hta1-S129A:ura4<sup>+</sup> hta2-S128A:his3<sup>+</sup> brc1::kanMX6 his3-D1 + pREP41XBrc1-W298F, P301G</i>
MR5474	<i>h<sup>-</sup> hta1-S129A:ura4<sup>+</sup> hta2-S128A:his3<sup>+</sup> brc1::kanMX6 his3-D1 + pREP41XBrc1-HYP307-9GFG</i>
MR5475	<i>h<sup>-</sup> hta1-S129A:ura4<sup>+</sup> hta2-S128A:his3<sup>+</sup> brc1::kanMX6 his3-D1 + pREP41XBrc1-T672A</i>
MR5477	<i>h<sup>-</sup> hta1-S129A:ura4<sup>+</sup> hta2-S128A:his3<sup>+</sup> smc6-74 his3-D1 + pREP41X</i>
MR5478	<i>h<sup>-</sup> hta1-S129A:ura4<sup>+</sup> hta2-S128A:his3<sup>+</sup> smc6-74 his3-D1 + pREP41XBrc1<sup>+</sup></i>
MR5479	<i>h<sup>-</sup> hta1-S129A:ura4<sup>+</sup> hta2-S128A:his3<sup>+</sup> smc6-74 his3-D1 + pREP41XBrc1-W298F, P301G</i>
MR5480	<i>h<sup>-</sup> hta1-S129A:ura4<sup>+</sup> hta2-S128A:his3<sup>+</sup> smc6-74 his3-D1 + pREP41XBrc1-HYP307-9GFG</i>
MR5481	<i>h<sup>-</sup> hta1-S129A:ura4<sup>+</sup> hta2-S128A:his3<sup>+</sup> smc6-74 his3-D1 + pREP41XBrc1-T672A</i>
MR5485	<i>h<sup>-</sup> hta1-S129A:ura4<sup>+</sup> hta2-S128A:his3<sup>+</sup> smc6-74 rhp18::hphMX6 his3-D1 + pREP41X</i>
MR5486	<i>h<sup>-</sup> hta1-S129A:ura4<sup>+</sup> hta2-S128A:his3<sup>+</sup> smc6-74 rhp18::hphMX6 his3-D1 + pREP41XBrc1<sup>+</sup></i>
MR5487	<i>h<sup>-</sup> hta1-S129A:ura4<sup>+</sup> hta2-S128A:his3<sup>+</sup> smc6-74 rhp18::hphMX6 his3-D1 + pREP41XBrc1-W298F, P301G</i>
MR5488	<i>h<sup>-</sup> hta1-S129A:ura4<sup>+</sup> hta2-S128A:his3<sup>+</sup> smc6-74 rhp18::hphMX6 his3-D1 + pREP41XBrc1-HYP307-9GFG</i>
MR5489	<i>h<sup>-</sup> hta1-S129A:ura4<sup>+</sup> hta2-S128A:his3<sup>+</sup> smc6-74 rhp18::hphMX6 his3-D1 + pREP41XBrc1-T672A</i>
MR5490	<i>h<sup>-</sup> natMX6:p41-13myc:Rhp18 brc1::kanMX6</i>
MR5491	<i>h<sup>-</sup> brc1::kanMX6 + pREP41-N-TAPbrc1<sup>+</sup></i>

MR5492 | *h natMX6:p41-13myc:Rhp18 brc1::kanMX6 + pREP41-N-TAPBrc1<sup>+</sup>*  
MR5493 | *h brc1::kanMX6 + pREP41-N-TAPbrc1-HYP307-9GFG*  
MR5494 | *h natMX6:p41-13myc:Rhp18 brc1::kanMX6 + pREP41-N-TAPBrc1-HYP307-9GFG*

543

544

545

546

547

## Figure 1

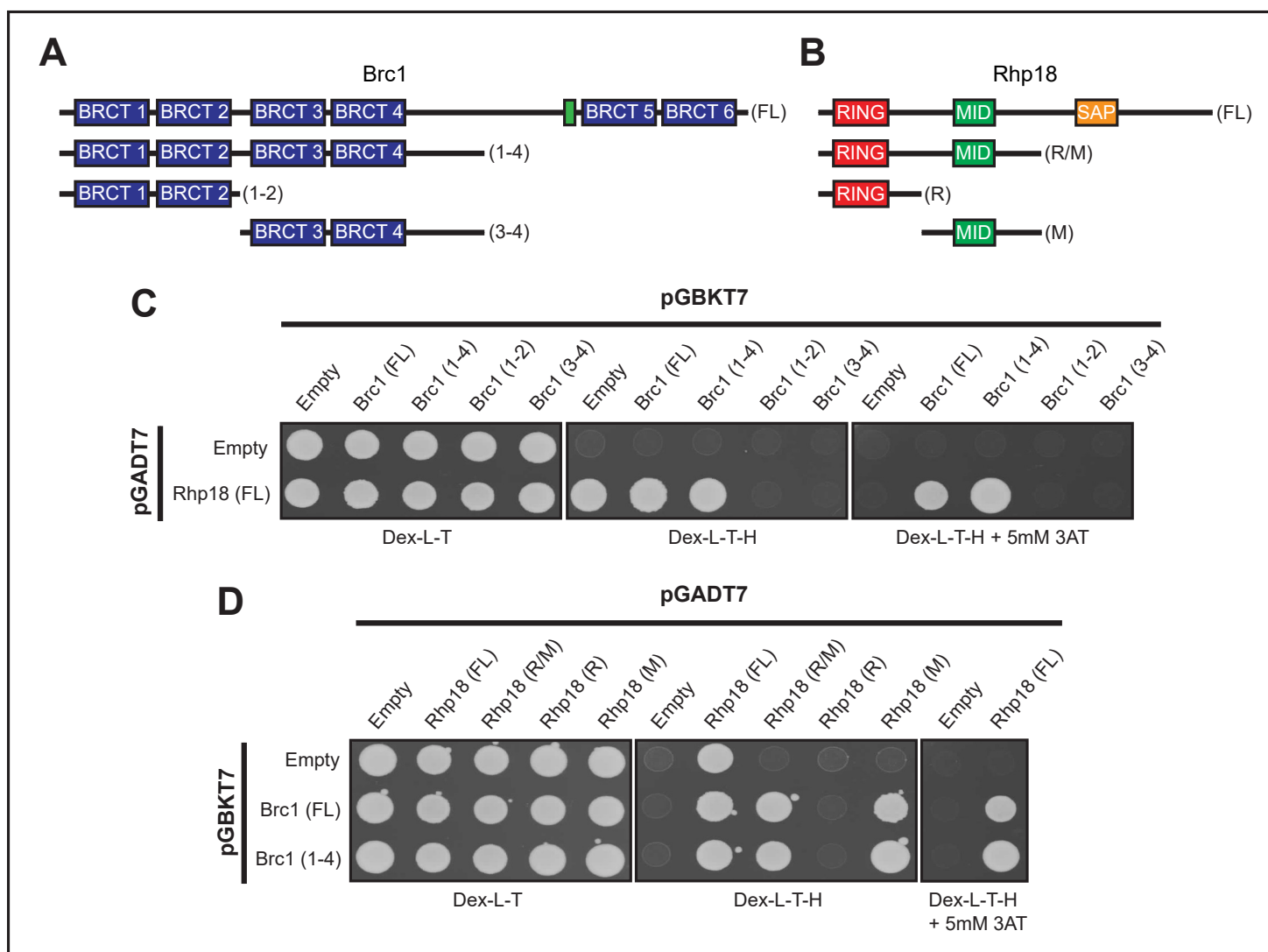


**Figure 1: The Brc1-Rhp18 interaction requires the N-terminal BRCT domains of Brc1 and the Mid domain of Rhp18.** **A** and **B**. Schematic representations of Brc1 (**A**) and Rhp18 (**B**) fragments tested for physical interactions by yeast two-hybrid analysis (fragments sizes for both Brc1 and Rhp18 are listed in the materials and methods section). The location of Brc1's nuclear localization signal is depicted by the green box in **A**. **C**. Yeast two-hybrid results showing full length Brc1 and BRCT domains 1-4 interact with full length Rhp18. Interactions were judged from the Dex-L-T-H+5mM 3AT due to observed one-hybrid activity of full length Rhp18 in pGADT7 on Dex-L-T-H. **D**. Yeast two-hybrid results indicating Rhp18's Mid domain is sufficient to support the interaction with Brc1. Interactions for full length Rhp18 were evaluated from the Dex-L-T-H+5mM3AT due to observed one-hybrid activity of full length Rhp18 in pGADT7 on Dex-L-T-H. Removal of the SAP domain of Rhp18 alleviated the observed one-hybrid activity, allowing assessment of physical interactions on Dex-L-T-H for the R/M, R, and M fragments of Rhp18.

## Figure 2

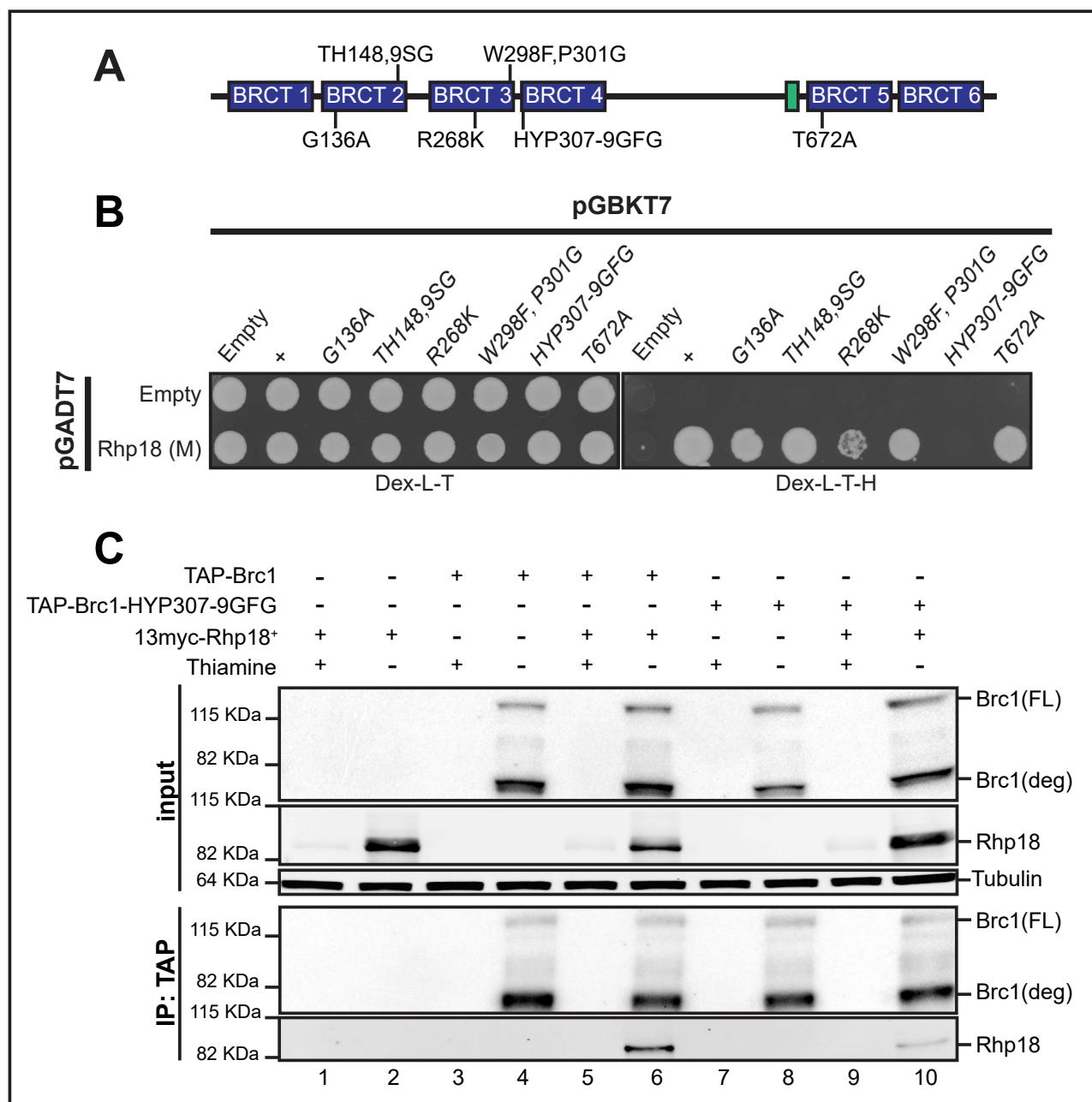


**Figure 2. Mutation of BRCT domain 4 attenuates the Brc1-Rhp18 interaction.**

**A.** A schematic representation of published Brc1 point mutations (Lee and Russell, 2013) tested for physical interaction with the Mid domain of Rhp18 by yeast two-hybrid analysis. **B.** Yeast two-hybrid results indicating that mutation of BRCT4 inhibits the interaction with the Mid domain of Rhp18.

**C.** Results from co-immunoprecipitation experiments demonstrating the interaction between full length Brc1 and Rhp18, as well as the reduction in Rhp18 binding observed with TAP-Brc1-HYP307-9GFG versus TAP-Brc1.

## Figure 3

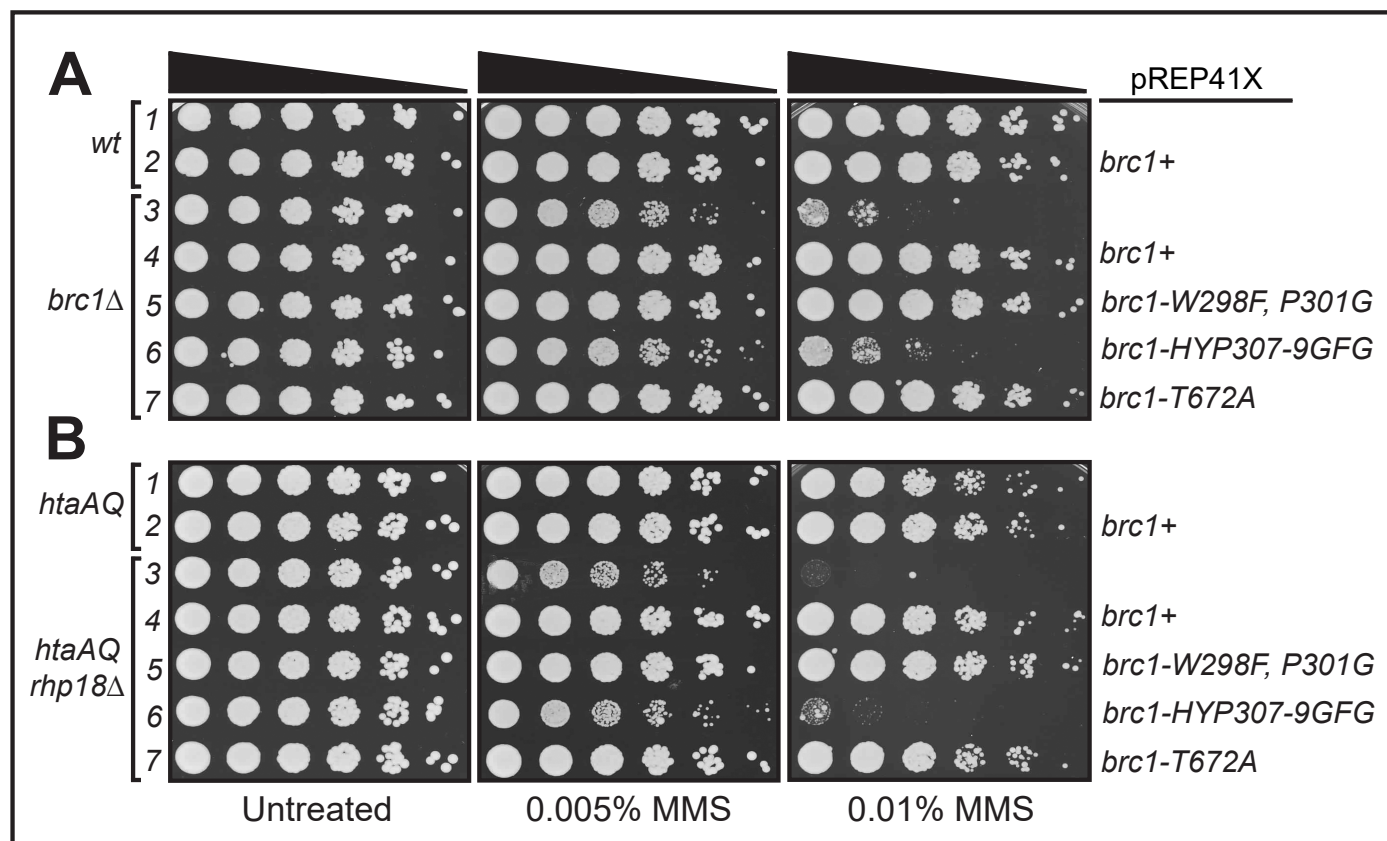


**Figure 3. Efficient rescue of *brc1* $\Delta$  by expression of *brc1*-T672A but not *brc1*-HYP307-9GFG.** **A.** Functional evaluation of four *brc1* alleles in response to MMS treatment in a *brc1* $\Delta$  genetic background suggests that *brc1*-HYP307-9GFG (Lee and Russell, 2013) retains more activity than *brc1* $\Delta$ , but significantly less than the previously published  $\gamma$ H2A binding mutant *brc1*-T672A (Williams, J., *et.al.*, 2010), which rescued *brc1* $\Delta$  as well as *brc1*<sup>+</sup> and *brc1*-W298F, P301G. **B.** Functional evaluation of the *brc1* alleles in response to MMS treatment in the *htaAQ* *brc1* $\Delta$  genetic background, demonstrating the Brc1-Rhp18 interaction is more essential for Brc1 function in an overexpression situation than its ability to bind  $\gamma$ H2A.

Figure 4

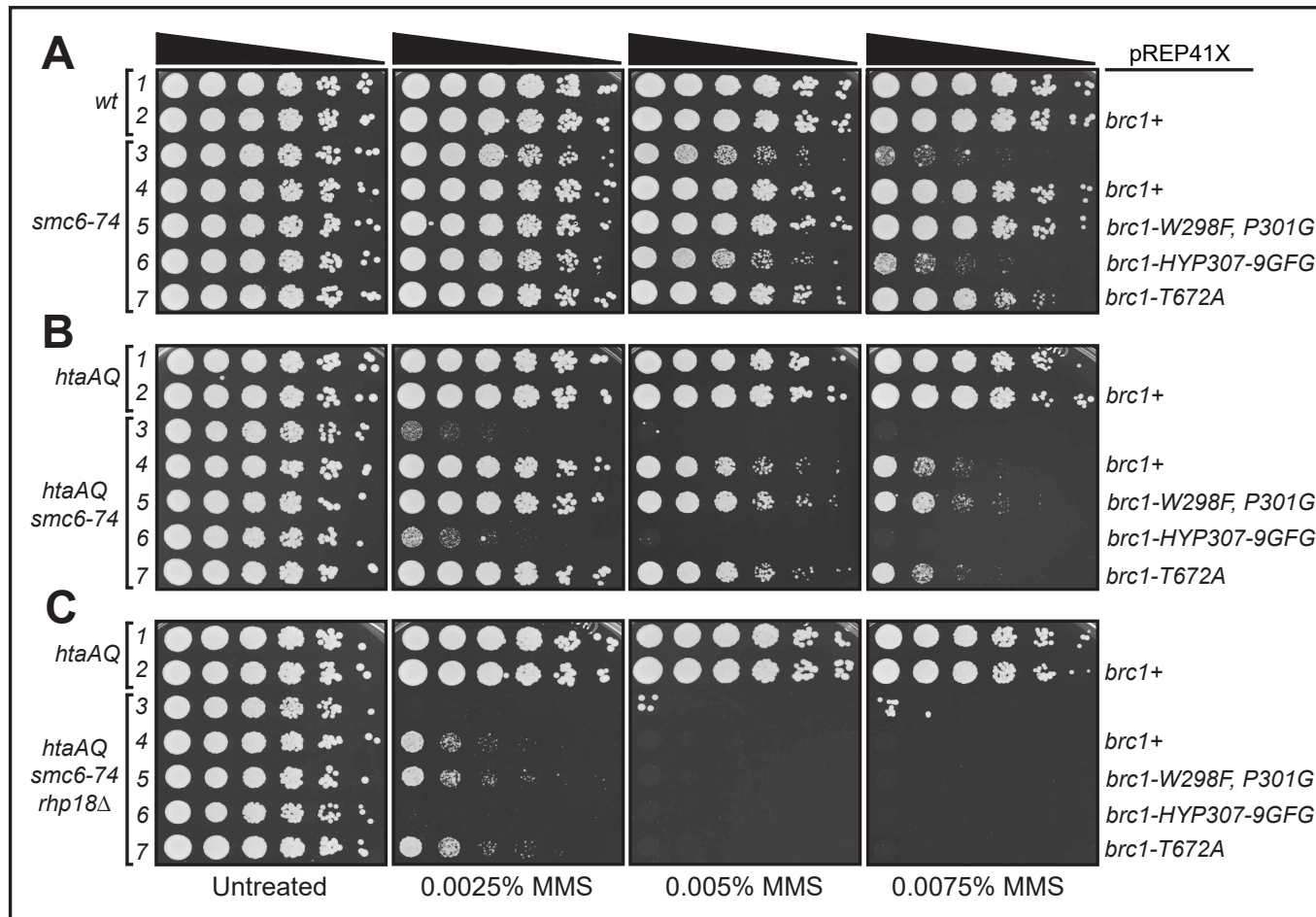


**Figure 4. Rhp18 and  $\gamma$ H2A binding are required for efficient rescue of *smc6-74* by Brc1 overexpression. A.** Results from *smc6-74* suppression experiments comparing the rescue efficiency of the four *brc1* alleles. The *brc1-HYP307-9GFG* allele that disrupts Brc1 binding to Rhp18 prevents Brc1 overexpression suppression of *smc6-74*. The *brc1-T672A* mutation that abrogates binding to  $\gamma$ H2A impairs Brc1 overexpression suppression of *smc6-74*. **B.** Results from *smc6-74 htaAQ* suppression experiments comparing the four *brc1* mutations, supporting the MMS dose dependence for  $\gamma$ H2A binding in mediating the *smc6-74* rescue by Brc1. **C.** Results from *brc1* overexpression assays in the *smc6-74 htaAQ rhp18Δ* background, suggesting the failure of *brc1-HYP307-9GFG* to rescue *smc6-74* is not completely explained by its inability to bind Rhp18.